Electronic Conductivity of Polypyrrole−Dodecyl Benzene Sulfonate Complexes

K. West, L. Bay,* and M. M. Nielsen

Danish Polymer Centre, Risø National Laboratory, DK-4000 Roskilde, Denmark

Y. Velmurugu[†] and S. Skaarup

Department of Chemistry, Technical University of Denmark, DK-2800 Lyngby, Denmark

Received: April 28, 2004; In Final Form: July 26, 2004

The electronic conductivity of the electroactive polymer polypyrrole−dodecyl benzene sulfonate (PPy−DBS) has been characterized as function of the redox level. The polymer was synthesized with different isomers of the dopant anions: the common mixed DBS tenside and three well-defined synthetic dodecyl isomers (with the benzene group at positions 1, 2 and 6). The conductivity was measured both by van der Pauw measurements on PPy−DBS in the oxidized, dry state as function of temperature, and by electrochemical impedance spectroscopy as function of potential in 0.1 M NaCl aqueous electrolyte. These investigations demonstrate that even minor differences in the dopant anion can cause significant changes in the physical properties of the electroactive polymer. The highest conductivities ($\sigma_{25} = 39$ Scm^{-1}) are obtained by the (6D)BS isomer, perhaps because the branching leads to denser packing and therefore smaller hopping distances. This was supported by X-ray measurements. Synthesis at lower temperatures generally leads to higher conductivity. The conductivity is strongly dependent on the potential, being more than four magnitudes smaller for the reduced state where the number of electronic carriers is at a minimum. The conductivity is further reduced because of the uptake of water at low potentials, creating electrolytic domains that separate the electronic domains and inhibit hopping. There is a pronounced hysteresis in the conductivity as a function of potential. However, the major part of this hysteresis can be accounted for by the composition hysteresis implying that that the conductivity mainly depends on the number of charge carriers, but not on the history of the sample.

Introduction

Conjugated polymers complexed with large anionic detergents show remarkably high stability in aqueous environments.[1] These materials are thus of interest for the development of new devices exploiting the special properties of conducting polymers.[2] One of the characteristic properties of these materials is their ability to be reversibly switched between a conducting (oxidized) and a nonconducting (neutral) state. During this switching many physical properties change dramatically, and this is the basis for the use of conjugated polymers as active materials in displays,[3] sensors,[4] and actuators.[5]

In this paper we report data on the changing electronic conductivity during redox switching of polypyrrole doped with different isomers of the anionic detergent dodecyl benzene sulfonate (PPy−DBS). Electronic conductivity is essential for the speed of the switching reaction, because the reaction requires the transport of electrons as well as of ions in the polymer matrix.

The method used in these investigations is in situ conductivity measurement, where the electronic conductivity is monitored while the redox state of the polymer is changed stepwise by changing the electrochemical potential. Other authors have previously described similar methods.[6,7] Here we use a slightly modified implementation, and a brief description of the method is included. Data for the temperature dependence of the conductivity of PPy−DBS in the dry, as-prepared (oxidized) state are also included as these give clues to the nature of the conduction mechanism.

Experimental Section

Pyrrole was distilled under nitrogen and stored cold and in the dark in capped vials prior to use. The synthesis electrolyte was 0.05 M in both pyrrole and sodium dodecyl benzene sulfonate. Three different isomers of the dopant ion were used: Na−4-(dodec-1-yl)-benzene−sulfonate (Na(1D)BS), Na−4-(dodec-2-yl)-benzene−sulfonate (Na(2D)BS), and Na−4-(dodec-6-yl)-benzene−sulfonate (Na(6D)BS). All were synthesized in-house according to literature procedures.[8] A commercial NaDBS (Aldrich) that is a complex mixture of several isomers and homologues was also used.

Constant current oxidation was used for polymer synthesis as this method provides the highest degree of control over the synthesis conditions. In our experience, this method yields well-defined polymers of a reproducible quality. A thermostat controlled the temperature of the synthesis solution. Samples were prepared at temperatures between 2 and 60 °C. For some of the isomers it proved impossible to make usable films in the full temperature range. When the synthesis temperature is below the Krafft point, only minor amounts of dopant ions can be dissolved in the electrolyte. The Krafft temperature was estimated to 58 °C for Na(1D)BS, 35 °C for Na(2D)BS, and 5−7 °C for Na(6D)BS, as the temperature where the conductivity of the tenside solutions changes abruptly on slow cooling. As NaDBS precipitates rather slowly, PPy−DBS synthesis can

* To whom correspondence should be addressed.

[†] Permanent address: Department of Physics, University of Peradeniya, Peradeniya, Sri Lanka.

10.1021/jp048153m CCC: $27.50
Published on Web 08/31/2004

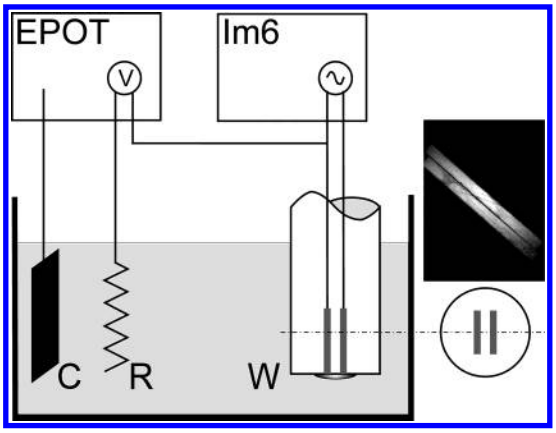

Figure 1. Experimental setup with a two-band working electrode used to determine the electronic conductivity of a conducting polymer as function of applied potential. The growth of PPy−DBS film across the gap is indicated. The distance between the two gold bands is greatly exaggerated. The inset photo micrograph shows the true relative dimensions of the 0.3-mm wide gold bands separated by the 18-μm insulating gap.

be performed in supercooled solutions below the Krafft point with some success. With Na(2D)BS homogeneous films could not be obtained at the highest synthesis temperature, 60 °C.

Free-standing polymer films were prepared by galvanostatic deposition onto a polished stainless steel electrode, after which the film could be peeled off the substrate. Unless otherwise stated, the polymerization current was 1 $mAcm^{-2}$ and the total charge deposited was 1600 $mCcm^{-2}$. The film thickness was measured with a DekTak profilometer and the proportionality between deposited charge and film thickness was shown to correspond to 160 $mCcm^{-2}$ per μm. The electronic conductivity of the dry film was calculated from the resistivity measured using the van der Pauw method[10] as a function of temperature in the interval from −35 to 80 °C. At each temperature the sample was allowed to equilibrate for 20 min before the measurement was taken. These measurements were performed in dry air (dew point approximately −50 °C). Samples were cut in cloverleaf shape to reduce systematic measuring errors.[11] Measurements over at least two subsequent temperature scans were recorded to make sure that irreversible changes in the film with time were not interpreted as temperature variations.

For the in situ conductivity measurements as a function of redox potential, PPy−DBS is deposited on a two-band gold electrode using a constant current of 1 mA per cm^2 of electrode area for 320−800 s, resulting in a PPy thickness of 2−5 μm. The in situ measurements are carried out in 0.1 M NaCl aqueous solutions bubbled with nitrogen to minimize the amount of dissolved oxygen. The two-band electrode consists of two pieces of gold foil, 0.3 mm wide, soldered onto gold wires. A 10-μm Kapton film is sandwiched between the Au foils and the laminate is subsequently embedded in epoxy resin (Specifix Resin, Struers A/S) in a PVC tube. The actual distance between the gold foils is 18 μm and includes thin resin layers at the Au−Kapton interfaces. One end of the assembly is ground and polished with emery paper #4000 until a smooth cross section of the epoxy-embedded Au foils is exposed. During polymerization the two gold foils are kept at the same potential (short-circuited), and because PPy has a propensity for growth along the nonconducting polymer surface, the insulating gap between the two gold foils is bridged by a PPy film during the initial stage of the polymerization.

The setup shown in Figure 1 is used to determine the conductivity of the deposited film as function of applied potential and consequently as a function of the redox state of the polymer. An auxiliary potentiostat (EPOT, Zahner) is operated in three-electrode configuration with the working electrode terminal (W) connected to one of the gold band electrodes, controlling its potential relative to a reference electrode (R, Ag/AgCl, 3 M KCl). The main potentiostat (IM6, Zahner) is connected in two-electrode configuration between the two gold band electrodes. The working electrode of the IM6 is connected to ground, while the EPOT is only grounded through the two-band electrode. A ground loop is thereby avoided, giving an improved signal-to-noise ratio.

Two different sets of impedance measurements are made. The conventional electrochemical impedance of the conducting polymer is obtained by keeping the two gold electrodes at the same potential (short-circuited through the IM6 potentiostat), while measuring the impedance with the auxiliary EPOT potentiostat relative to a reference electrode in the frequency range from 100 kHz to 25 mHz (50 mV amplitude). The composition-dependent conductivity of the PPy film is measured in another measurement type, where the IM6 potentiostat applies a sinusoidal voltage difference (20 mV amplitude, frequency range from 25 kHz to 100 mHz) between the two gold electrodes while the overall redox state of the conducting polymer is controlled with the dc level on the auxiliary potentiostat. The setup is software controlled, which allows for automatic shifting between the two kinds of impedance measurement and subsequent stepping of the electrochemical redox state of the PPy. Data series with a potential step of 50 mV and a rest time of 1000 s after each potential change were collected. In a full measurement cycle the potential was stepped from 0.3 V vs Ag/AgCl down to −0.85 V vs Ag/AgCl and back again.

The cell constant of the polymer-coated two-band electrode cannot be determined a priori because the thickness of the polymer is not constant across the gap between the gold bands (Figure 1), and because imperfect bridging is occasionally observed. In particular, the affinity to grow along the surface was observed to be lower for PPy(2D)BS at 30 °C, and as mentioned above, this system does not form coherent films at all at 60 °C. The cell constant for each polymer preparation was calibrated by comparing the resistance of the dry, as-coated two-band electrode with the resistivity of the free-standing PPy films prepared under identical conditions.

The structure of the samples was investigated by grazing incidence wide-angle X-ray scattering (WAXS). The setup uses a rotating anode (Cu target, 18 kW Rigaku), and allows for the concurrent acquisition of a large section of the two-dimensional distribution of scattered intensity. Using an imaging plate to collect the scattered intensity ensures a high dynamic range. The samples used in these experiments are 0.1−0.5-μm films polymerized onto gold-covered silicon wafers.

Results and Discussion

The conductivity of conjugated polymers increases with temperature, because the electron transport is facilitated by a hopping mechanism. The temperature-dependent conductivity for different hopping mechanisms can be expressed as[12]

$$\sigma = \frac{K_0}{T^b} \cdot \exp[-(T_0/T)^\gamma] \qquad (1)$$

or as

$$\sigma = \sigma_0 \cdot \exp[-(T_0/T)^\gamma] \qquad (2)$$

TABLE 1: Conductivity Parameters for Dry PPy−DBS Films with Different DBS Isomers. Conductivity at 25 °C: σ_{25}; Activation Energy: E_a (eq 3) and T_0 (eq 4)

synthesis temperature	Aldrich		PPy−(6D)BS			PPy−(2D)BS		PPy−(1D)BS	
	$\sigma_{25}/(\Omega\text{cm})^{-1}$	E_a/meV	$\sigma_{25}/(\Omega\text{cm})^{-1}$	E_a/meV	T_0/kK	$\sigma_{25}/(\Omega\text{cm})^{-1}$	E_a/meV	$\sigma_{25}/(\Omega\text{cm})^{-1}$	E_a/meV
5 °C	8	38	24	21	4.9				
25 °C	10	33	39	26	8.5	17[a]	28[a]		
60 °C	5	41	20	29	12.9			7	38

[a] Synthesized at 30 °C.

emphasizing the fact that the major part of the temperature dependence stems from the exponential term. When describing electron hopping between fixed sites, γ is equal to unity and eq 2 is then equivalent to the Arrhenius expression:

$$\sigma = \sigma_0 \cdot \exp(-E_a/kT) \tag{3}$$

where E_a is the height of the energy barriers separating the sites ("activation energy"). In disordered media, variable range hopping (VRH) models[13] with $\gamma < 1$ can be applied. The value of γ is related to the dimensionality of the transport process. For three-dimensional jumping paths (in the absence of strong Coulombic interactions between the moving particles), the VRH model predicts $\gamma = 1/4$ and $b = 1/2$.

The constants K_0 and T_0 depend on the decay length of the wave function of the localized states and on the density of states near the Fermi level.[13]

For conduction in conjugated polymers, both fixed range and variable range[14,15] hopping have been used to describe the observed temperature dependence of the conductivity. Wegner and Rühe[16] point out that a crossover from VRH at low temperatures to Arrhenius behavior at high temperatures may be expected. Alternatively, models describing the polymer medium as made up of highly conducting islands separated by insulating barriers have in some cases been used to describe deviations from VRH or Arrhenius behavior.[15,17,18]

Baughman et al.[19] analyzed the dependence of the electronic conductivity of conducting polymers on the conjugation length. For polymers having relatively short conjugation lengths, they predicted a temperature dependence that can be described by eq 2 with $\gamma = 1/3$, based on a model involving nearest-neighbor hopping with a distribution of activation energies stemming from a distribution of conjugation lengths:

$$\sigma = \sigma_0 \cdot \exp[-(T_0/T)^{1/3}] \tag{4}$$

The parameter T_0 in their model is inversely proportional to the weight average number of monomers in the conjugated segments.

Conductivity of Dry Polymer Foils. Figure 2 shows the results from van der Pauw measurements of the electronic dc conductivity of a dry PPy−(6D)BS sample in the temperature range −35 to 75 °C. The conductivity during the first heating typically shows a different behavior from what is seen in later thermal cycles. After an equilibration period at 75 °C, the subsequent cooling and heating curves follow the same straight line in the Arrhenius plot. During the first heating an equilibrium state is apparently reached, either because water is leaving the film or because a more stable polymer configuration is established through annealing. The experimental data are modeled well by the Arrhenius eq 3, but are modeled slightly better by the distributed conjugation length model, eq 4. In the limited temperature interval investigated here, the difference in the quality of the fits is not really significant. The conductivity and activation energy data are listed in Table 1 for commercial DBS and for the custom-synthesized DBS isomers. For all

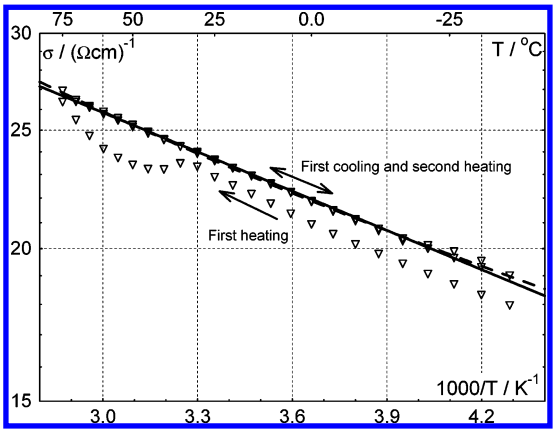

Figure 2. Electronic conductivity of dry PPy−(6D)BS (synthesized at 5 °C) measured in the temperature interval from −35 to 75 °C. The solid line is a fit to the Arrhenius eq 3 and the broken line to eq 4.

preparations, the conductivity of PPy−DBS films showed a relatively small temperature variation or a low value of the activation energy for electron transport. This is consistent with findings for PPy with other dopants. Yamaura et al.[20] reported activation energies close to 10 meV for electrochemically synthesized PPy doped with either perchlorate or tosylate in propylene carbonate. From the graph in Tsutsumi et al.,[21] the activation energy can be estimated to 40 meV in the temperature interval between 0 and 100 °C for PPy−ClO_4 synthesized under similar conditions.

It is seen from the data in Table 1 that the nature of the anionic detergent incorporated into the polymer during synthesis has influence on the conductivity of the complex. In general, (6D)BS yields polymers with a higher conductivity and a lower activation energy than the mixed isomer commercial DBS. The two other isomers, (2D)BS and (1D)BS, can only be used for synthesis in a narrow temperature interval, but the polymer complexes made with these are also less conducting than PPy−(6D)BS. The influence of the synthesis temperature is less clear. It should be noted that the data in Table 1 represent a number of different synthesis series made in different laboratories and by different experimentators. The observed difference between nominally identical polymers is not much smaller than the differences observed by changing the synthesis temperature. There is, however, a tendency for an increase in the activation energy with increasing synthesis temperature, and the conductivity of the samples prepared at 60 °C are often relatively low. This variation can be understood in terms of polymer perfection. In the samples prepared at lower temperatures, the polymer chain segments with ideal conjugation are longer, leading to a higher conductivity. Preparation at higher temperatures leads to the formation of more defects acting as barriers between the conducting conjugated polymer segments. This will increase the overall activation energy and decrease the conductivity. The fit to Baughman's model for the PPy−(6D)BS data indicates that the conjugation length of the polymer prepared at 5 °C is more than twice as long as when the polymer is prepared at 60 °C.

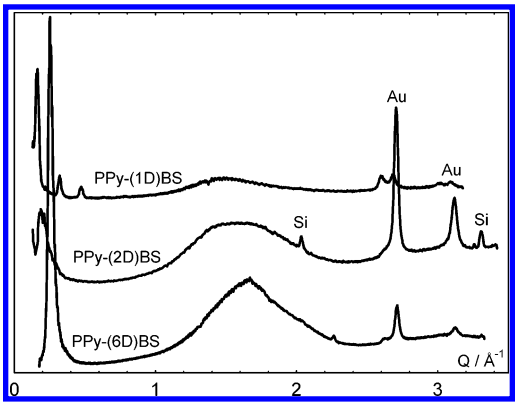

Figure 3. Integrated grazing incidence out-of-plane scattering intensities of PPy−(xD)BS on gold coated silicon wafers.

However, this tendency is opposed by the slower kinetics at lower temperatures. As the syntheses in Table 1 are all driven by the same current density, synthesis at the lower temperatures will be more prone to limitations by kinetics and thus show a larger fraction of defects caused by a higher synthesis overvoltage. At 5 °C we actually did see a significant increase in conductivity with decreasing synthesis current. For thinner PPy−DBS preparations we observed an increase from $\sigma_{25} = 6.4$ $(\Omega\text{cm})^{-1}$ for polymers synthesized at 1 mAcm^{-2} to $\sigma_{25} = 13.5$ $(\Omega\text{cm})^{-1}$ for polymers synthesized at 0.1 mAcm^{-2}, supporting the kinetic limitation.

The higher conductivity of PPy−(6D)BS is consistent with structural investigations showing the lowest *d*-values for this material. Figure 3 shows the out-of-plane scattering intensities for PPy−(1D)BS, PPy−(2D)BS, and PPy−(6D)BS. The broad scattering peak at *q*-vectors between 1 and 2 Å^{-1} corresponds to in-chain pyrrole−pyrrole distances, but a peak at low *q*-vectors can be interpreted as the stacking distance between polymer chains. From these peaks a *d*-value can be estimated: PPy−(1D)BS: $d = 39.2$ Å, PPy−(2D)BS: $d = 31.7$ Å, and PPy−(6D)BS: $d = 24.2$ Å. These data are not sufficient to support a model for the structure of PPy−DBS, but it can be seen that the *d*-values increase with the length of the longest alkyl chain in the DBS anion. This indicates that the alkyl chains in PPy−DBS are in a relatively stretched configuration. By itself, the shorter interchain distance will give rise to a higher conductivity.

Electrochemical Switching of PPy−DBS. The process of switching polypyrrole doped with large anionic detergents between the oxidized and the neutral states has very complex dynamics. Figure 4 shows a voltammogram of PPy−(6D)BS cycled in 0.1 M NaCl. The lack of symmetry between the anodic and cathodic currents does not disappear on going to lower sweep-rates, but is an indication of an inherent hysteresis in this process. Detailed studies of the switching process have shown that cations, anions, and solvent move in and out of the polymer during the switching process, and the hysteresis has been linked to slow relaxation processes involving conformation changes of the polymer chains in response to changes in the density of charge and solvent in the polymer matrix.[22,23]

Impedance of the Two-Band Electrode. An electrical model for the PPy−DBS-coated two-band electrode is illustrated in Figure 5A. When measuring in the three-electrode configuration the reaction impedances Z_R will dominate, as the size of the gap is small compared to the width of the gold electrodes (figure not to scale). The measured electrode impedance, Z_{ec}, will be a parallel connection of the two Z_R elements, $Z_{ec} = Z_R/2$. On the other hand, in the configuration where the impedance between

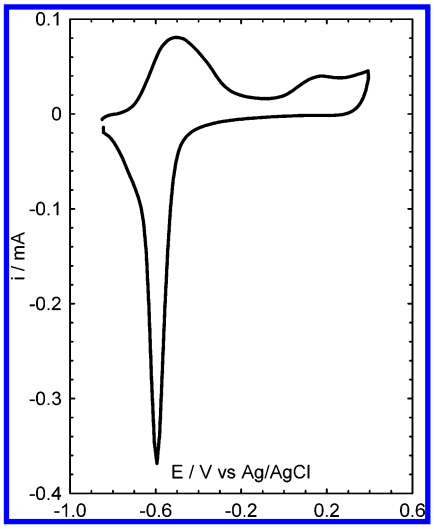

Figure 4. Cyclic voltammogram of PPy−(6D)BS on Pt (area 0.2 cm^2, thickness 0.5 μm). Sweep rate: 25 mV/s, electrolyte: 0.1 M NaCl.

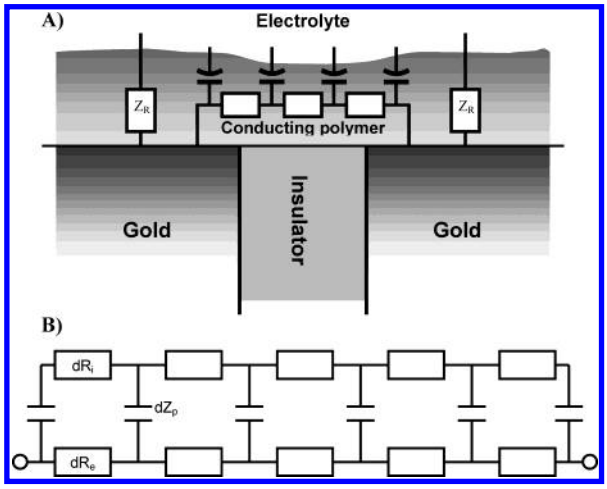

Figure 5. (A) Equivalent circuit model description of a two-band electrode covered with a conducting polymer layer and immersed in electrolyte. Z_R is the reaction impedance. (B) Generalized form of the network circuit (impedance: Z_N), connecting the two gold electrodes across the gap when polymer is present. R_i and R_e represent the interacting ionic and electronic resistances. Z_p is the capacitive impedance between the branches.

the two-band gold electrodes, Z_{2B}, is measured, the network (impedance Z_N) connecting the two electrodes in Figure 5A will dominate the low-frequency impedance as Z_R is predominantly capacitive and thus blocking at low frequencies. The resistive chain represents the electronic conduction path between the two gold electrodes. In each volume element, electrons can participate in the polymer redox reaction, defining the charge on the polymer backbone. This is illustrated by the capacitive elements in the figure. Through these elements electrons interact with ionic species in the electrolyte. In Figure 5B this network impedance element, Z_N, is generalized to include the distributed electrolyte resistance. The impedance of this equivalent circuit is given by[24]

$$Z_N = \frac{R_e^2}{R_e + R_i}\frac{\tanh(\alpha(\omega))}{\alpha(\omega)} + \frac{R_e R_i}{R_e + R_i}, \quad \alpha(\omega) = \frac{1}{2}\sqrt{\frac{R_e + R_i}{Z_p(\omega)}} \tag{5}$$

R_e is the integral resistance in the lower branch (electronic conduction), R_i in the upper branch (ionic conduction), and Z_p

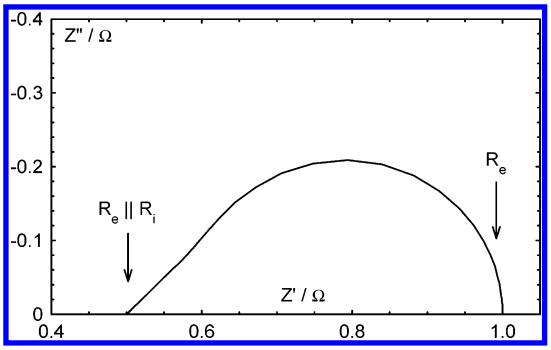

Figure 6. Simulated impedance response of the ladder network shown in Figure 5B assuming that Z_p is capacitive and that $R_e = R_i = 1\ \Omega$.

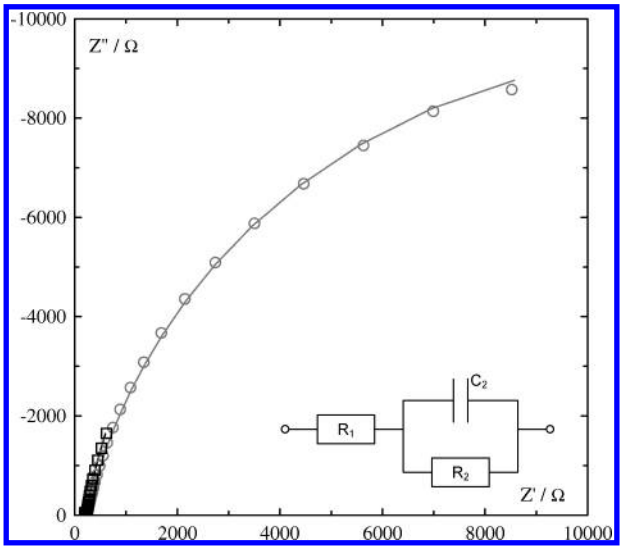

Figure 7. Complex impedance plot of PPy(6D)BS (synthesized at 2 °C) in 0.1 M NaCl measured against the Ag/AgCl reference electrode, circles at 0.00 V (high conductivity), and squares at −0.75 V (low conductivity). The solid curves are simulated curves based on the equivalent circuit shown as an insert on the figure.

is the integral (capacitive) impedance between the branches. In a Cole−Cole plot Z_N is roughly represented by an arc spanning the parallel combination of the ionic (R_i) and electronic (R_e) resistances, $(R_e^{-1} + R_i^{-1})^{-1}$ to R_e, see Figure 6.

In the potential region where the polymer conducts well, Z_{2B} will be very close to Z_N. But, when R_e increases to a magnitude where Z_N becomes comparable to Z_R, the shunting through the electrolyte can cause Z_{2B} to deviate from Z_N. In the present case, the electrochemical impedance of the electrode, Z_{ec}, is determined experimentally, and the effect of the shunt can be assessed by assuming that the impedance of the shunt is $2*Z_R$. The value of Z_N can then be found from the measured impedances by

$$Z_N = \left(\frac{1}{Z_{2B}} - \frac{1}{4*Z_{ec}}\right)^{-1} \quad (6)$$

In a real electrode the current pathway through the shunt will be frequency dependent, and eq 6 above will thus only be used to estimate the magnitude of the error incurred by assuming that Z_N is equal to Z_{2B}. The electronic resistance, R_e, is extracted from the experimental data as the low-frequency limit of the Z_{2B} impedance trace or by using conventional nonlinear least-squares analysis.[25]

Electrochemical Impedance. Figure 7 shows the frequency variation of the high-frequency (100 Hz−100 kHz) impedance of a PPy−(6D)BS covered two-band electrode measured against the reference electrode. This is the frequency range where electron mobility can be expected to contribute significantly to the electrode admittance. At lower frequencies ionic mobility becomes significant and will totally dominate the admittance. As illustrated in the figure, the measured impedances in this frequency interval form part of a semicircle in the impedance plane. Consequently, the high-frequency impedance can be modeled by the equivalent circuit shown as an insert in Figure 7. The potential variations of the equivalent circuit parameters for PPy−(6D)BS are shown in Figure 8. The high-frequency intercept, R_1, is nearly constant at potentials above −0.6 V vs Ag/AgCl where the polymer is in the doped, conducting state. At lower potentials the resistance first rises and then drops off to the high potential level at −0.8 V. This is somewhat different from previous findings in nonaqueous electrolytes[26] where the high-frequency intercept increases to a higher level at low potentials because reduction of the polymer leads to an increased resistance of the polymer layer. It is known from other investigations that PPy−DBS in the reduced form contains a large amount of ions and solvent,[27] and the drop in R_1 at low potentials shows that the ionic conductivity in the electrolyte-swollen material effectively shunts the electronic conducting

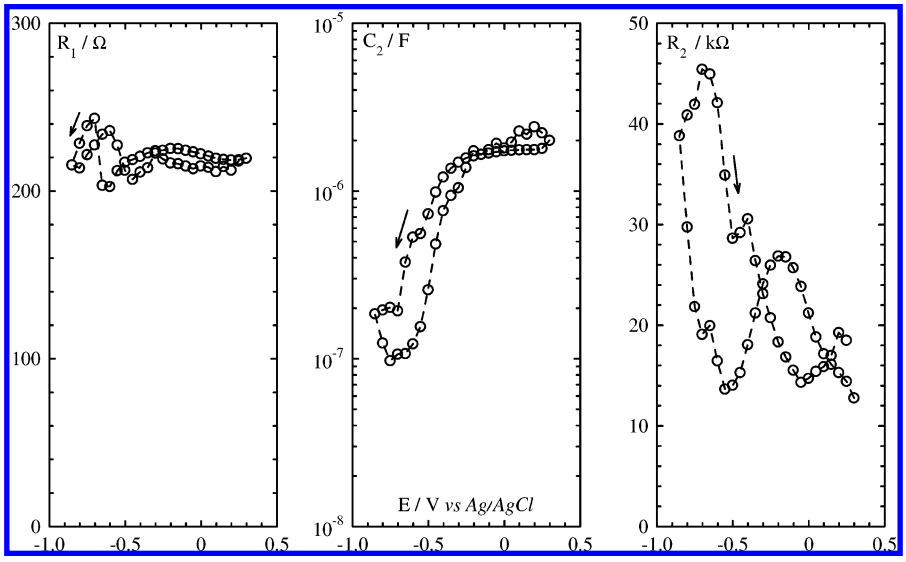

Figure 8. Equivalent circuit parameters for the high-frequency part of the impedance of PPy(2D)BS fitted to the equivalent circuit shown as an insert in Figure 7.

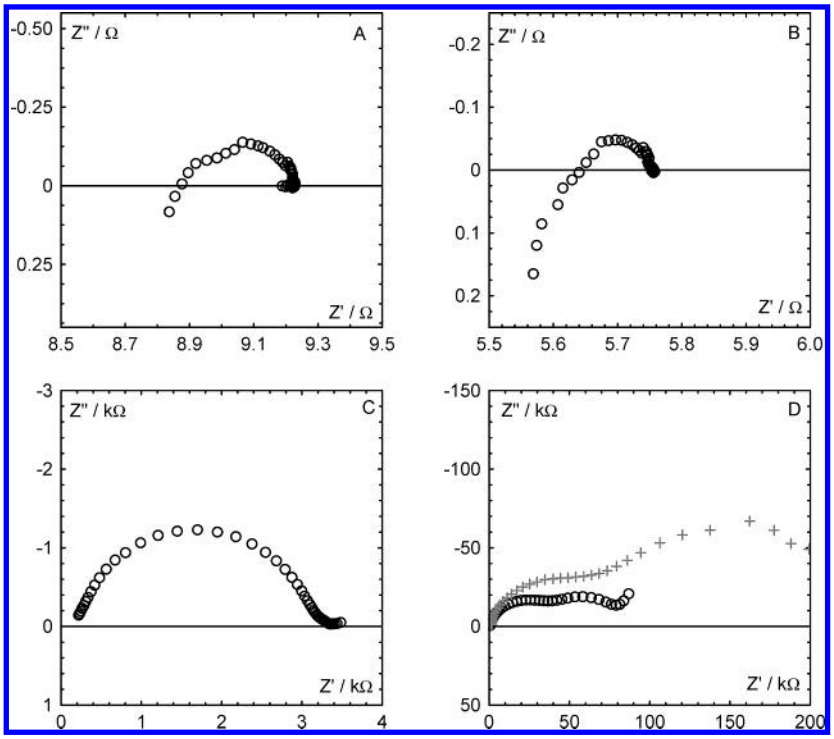

Figure 9. Complex impedance plot of PPy(6D)BS (synthesized at 2 °C) in 0.1 M NaCl measured between the two-band-electrodes. The potential of the electrode against the Ag/AgCl reference electrode: A: 0.25 V; B: −0.25 V; C: −0.60V; D: −0.75 V. The impedances are measured in the frequency interval between 25 kHz and 0.1 Hz. The crosses in D shows the impedance corrected for the shunting by the reaction impedance, Z_R.

path at high frequencies. The parallel capacitance, C_2, shows a clear potential dependence, being more than an order of magnitude smaller at low potentials where the polymer is expected to be nonconducting and where the number of free carriers in the polymer no longer changes with potential. The parallel resistor, R_2, shows a complex potential variation corresponding to the equally complex dynamics of polymer relaxation. The overall trend is that the resistance is highest at low potentials where the reaction is linked to conformation changes in the polymer.

Electronic Conductivity. Two-band impedances of PPy−(6D)BS synthesized at 2 °C and measured at different electrode potentials are shown in Figure 9. At higher electrode potentials (E > −0.65 V vs Ag/AgCl) the impedance trace follows the expected semicircular shape, and because of the low impedance values the contribution from the Z_R shunt is negligible. At lower potentials the response is characterized by two time constants. The additional time constant is not due to the shunt through Z_R as can be seen from Figure 9D, where the measured impedance is corrected for this contribution using the experimentally determined three-electrode electrochemical impedance. There are two possible explanations for the additional time constant. One is the appearance of an ohmic contact between the metallic gold electrode and the semiconducting PPy−DBS. This explanation is, however, not very likely because of the relatively long time constants involved (e.g., approximately 1 s for the new low-frequency semicircle at −0.75 V vs Ag/AgCl increasing to 10 s at −0.85 V). Alternatively, it could be the electronic conduction process itself that gives rise to the two time constants: one associated with conduction through highly conjugated domains and one associated with electrons passing from one domain to the next. In addition to the low-frequency semicircle, a low-frequency spike is appearing in the two-band measurements on PPy−(6D)BS at potentials below −0.7 V vs Ag/AgCl.

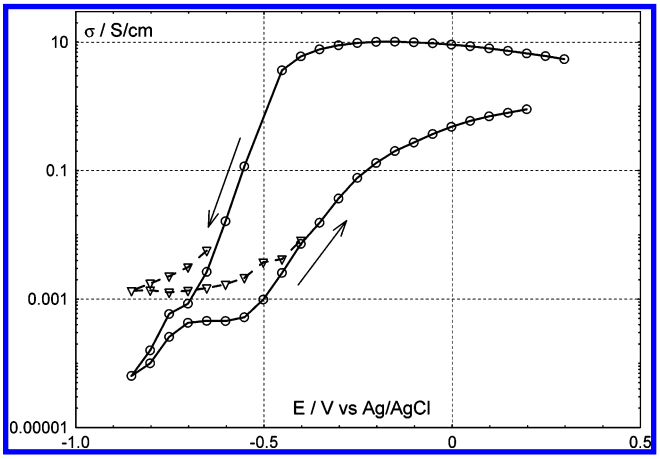

Figure 10. Electronic conductivity of PPy−(6D)BS synthesized at 2 °C. The data are based on two-band electrode measurements and are given as function of the electrode potential. The triangles correspond to the purely electronic contribution with the shorter time constant identified in Figure 9.

By comparing the value of R_e for the dry as-prepared electrode with the electronic conductivity of a similarly prepared polymer film, the cell constant of the polymer-covered two-band electrode can be determined, and the electronic conductivity can be calculated as function of the applied potential, see Figure 10. At low potentials where the response is characterized by an additional time constant, both the total extrapolated dc conductivity and the conductivity calculated from the faster relaxation are shown. Whereas the conductivity contribution associated with the shorter time constant (close to 10 ms) approaches a constant value at E < −0.7 V vs Ag/AgCl where the polymer reaches the uncharged, semiconducting state, the second contribution causes the combined conductivity to decrease further in this range. This is consistent with the interpretation proposed above for the high-frequency three-electrode impedances based on the assumption that the polymer

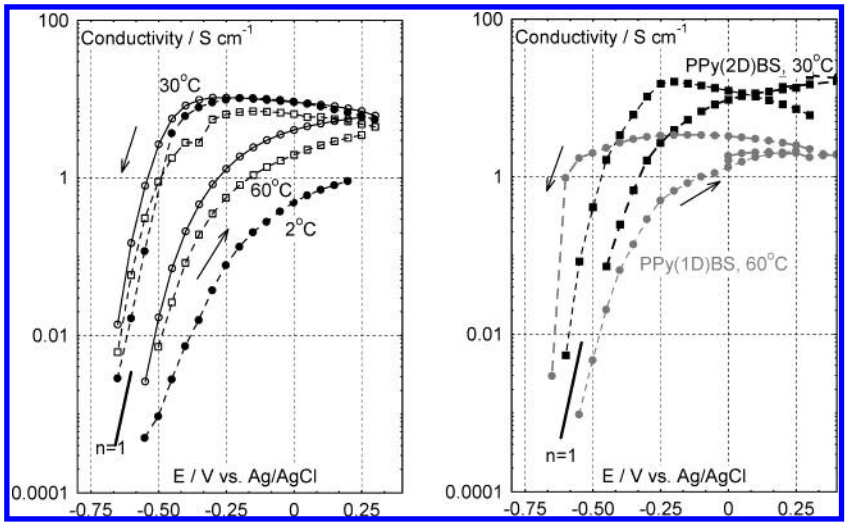

Figure 11. Electronic conductivity of PPy(xD)BS prepared at different temperatures vs the redox potential. Left: PPy(6D)BS polymerized at 2, 30, and 60 °C. Right: PPy(2D)BS polymerized at 30 °C and PPy(1D)BS polymerized at 60 °C. The inserted straight lines correspond to the change in the number of charge carriers following the Nernst equation.

swells at these potentials, and that the swollen, ion-conducting regions penetrate the electron-conducting conjugated regions. The low-frequency spike that blocks dc-conduction at potentials below −0.7 V vs Ag/AgCl shows that the electronically conducting domains at these potentials becomes isolated from each other by the electrolytic domains.

The electrodes prepared at higher temperatures show time-dependent changes at low potentials, and the low-frequency impedance is more noisy and cannot be analyzed in the same detail. The second time constant is less well resolved and the low-frequency spike more dominating, but basically the patterns are the same as described above. In Figure 11 the calculated electronic conductivities for the different PPy−DBS syntheses are compiled. Only data based on two-band impedances with a single semicircular trace are included. It can be seen that all materials follow the same pattern, with a conductivity drop of approximately four orders of magnitude at negative potentials and a large hysteresis between the data measured during the negative potential scan and during the positive scan. It is also seen that the maximum conductivity is not attained at the maximum doping density, but rather at an intermediate doping level where doping with mobile anions has not started yet and where the amount of solvent swelling is at a minimum.[23] The electronic conductivity of the electrolyte swollen polymer is generally lower than of the dry as-prepared PPy−DBS. The reduction on soaking is smallest for PPy-(2D)BS, which show higher electronic conductivity in the wet state than PPy−(6D)BS, probably because of a lower water uptake.

The logarithm of the conductivities changes almost linearly with the potential at negative potentials. The slope is close to the value obtained by assuming that the charge carriers have constant mobility and that their number follows the Nernst equation. This slope is indicated with straight lines in the figure. The synthesis temperature does not influence the slope. Alternatively, the potential dependence of the doping level can be estimated from cyclic voltammograms on similar electrodes. Based on the voltammogram shown in Figure 4, the composition dependence of the conductivity is estimated and shown in Figure 12. It can be seen that the major part of the apparent hysteresis in Figure 10 disappears by this transformation. The remaining difference between conductivities in the anodic and the cathodic scans can be ascribed to the uncertainty in the composition determination.

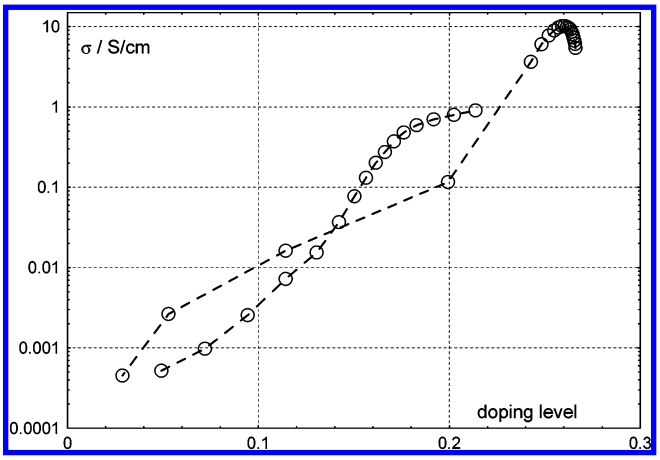

Figure 12. Conductivity of PPy−(6D)BS plotted vs composition given as the doping level, *x*, of PPy^{x+}. The doping level is calculated from the voltammogram in Figure 4.

Conclusion

The electronic conductivity of different preparations of PPy−DBS has been measured. The temperature variation of the conductivity of dry, doped samples is well described by the model based on nearest-neighbor hopping proposed by Baughman.[19] There is a tendency for the polymers prepared at lower temperature to have higher conductivities and lower activation energies, showing that the lower synthesis temperature leads to more perfect conjugation. Because of the slower kinetics at lower temperature, it is necessary, however, to reduce the synthesis current, which makes synthesis at low temperatures very time-consuming.

The highest conductivities are obtained with PPy−(6D)BS. Possibly because the branching leads to denser packing and therefore smaller hopping distances, this is supported by WAXS measurements, showing that the interchain distance in PPy−(6D)BS is 24.2 Å compared to 39.2 Å in PPy−(1D)BS and 31.7 Å in PPy−(2D)BS. There is a distinct advantage in terms of conductivity to be gained on replacing the conventional mixture of homologues with this more well-defined tenside.

The electronic conductivity was measured in situ during switching of PPy−DBS between the oxidized, conducting state, and the neutral, semiconducting or nonconducting states. During the switching, the conductivity changes approximately four

orders of magnitude. In the neutral state, where the conjugated domains become semiconducting, osmotic effects cause the polymer to take up a considerable amount of water, and the two-band measurements indicate that this causes the formation of electrolytic domains in the polymer. These ionic conducting domains separate the semiconducting electronic domains, thereby further reducing the dc electronic conductivity of the polymer. The conductivity at a given potential is dependent on whether this potential is reached from the negative or positive side. However, the major part of this hysteresis can be accounted for by the composition hysteresis implying that that the conductivity mainly depends on the number of charge carriers, but not on the history of the sample.

Acknowledgment. The financial assistance to Y. Velmurugu from IPPS (International Programs of Physical Sciences), Uppsala University, Sweden, is gratefully acknowledged.

References and Notes

(1) Kudoh, Y.; Akami, K.; Matsuya, Y. *Synth. Met.* **1998**, *95*, 191.
(2) Bay, L.; West, K.; Sommer-Larsen, P.; Skaarup, S.; Benslimane, M. *Adv. Mater.* **2003**, *15*, 311.
(3) Yang, Y. *MRS Bull.* **1997**, *22*(6), 31.
(4) Barisci, J. N.; Lewis, T. W.; Spinks, G. M.; Too, C. O.; Wallace, G. G. *J. Intell. Mater. Syst. Struct.* **1999**, *9*, 723.
(5) Baughman, R. H. *Synth. Met.* **1996**, *78*, 339−353.
(6) Schiavon, G.; Sitran, S.; Zotti, G. *Synth. Met.* **1989**, *32*, 209−17.
(7) Holze, R.; Lippe, J. *Synth. Met.* **1990**, *38*, 99.
(8) Bay, L.; Mogensen, N.; Skaarup, S.; Sommer-Larsen, P.; Jørgensen, M.; West, K. *Macromolecules* **2002**, *35*, 9345.
(9) Kruszka, J.; Nechtschein, M.; Santier, C. *Rev. Sci. Instrum.* **1991**, *62*, 695−699.
(10) van der Pauw, L. J. *Philips Res. Rep.* **1958**, *13*, 1−9.
(11) Koon, D. W. *Rev. Sci. Instrum.* **1988**, *60*, 271−274.
(12) Capaccioli, S.; Lucchesi, M.; Rolla, P. A.; Ruggeri, G. *J. Phys.: Condens. Matter* **1998**, *10*, 5595−5617.
(13) Mott, N. F.; Davis, E. A. *Electronic Processes in Non-Crystalline Materials*; Clarendon Press: Oxford, 1971.
(14) Kaynak, A. *Mater. Res. Bull.* **1998**, *33*, 81−88.
(15) Kemp, N. T.; et al. *J. Polym. Sci. Part B* **1999**, *37*, 953−60.
(16) Wegner, G.; Rühe, *J. Faraday Discuss. Chem. Soc.* **1989**, *88*, 333−349.
(17) Dyreklev, P.; Granstrom, M.; Inganaes, O.; Gunaratne, L. M. W. K.; Senadeera, G. K. R.; Skaarup, S.; West, K. *Polymer* **1996**, *37*, 2609−2613.
(18) Waage, B.; Schlüter, A.-D.; Leising, G. *Synth. Met.* **1997**, *84*, 933.
(19) Baughman, R. H.; Shacklette, L. W. *Phys. Rev. B: Condens. Matter* **1989**, *39*, 5872−5886.
(20) Yamaura, M.; Sato, K.; Hagiwara, T. *Synth. Met.* **1990**, *39*, 43−60.
(21) Tsutsumi, N.; Ishida, S.; Kiyotsukuri, T. *J. Polym. Sci., Part B: Polym. Phys*. **1994**, *32*, 1899−1906.
(22) Skaarup, S.; Bay, L.; Vidanapathirana, K.; Thybo, S.; Tofte, P.; West, K. *Solid State Ionics* **2003**, *159*, 143−7.
(23) Vidanapathirana, K. P.; Careem, M. A.; Skaarup, S.; West K. *Solid State Ionics* **2002**, *154−155*, 331−335.
(24) Albery, W. J.; Elliott, C. M.; Mount, A. R. *J. Electroanal. Chem.* **1990**, *288*, 15−34.
(25) Boukamp, B. A. *Solid State Ionics* **1986**, *20*, 31.
(26) West, K.; Careem, M. A.; Skaarup, S. *Solid State Ionics* **1993**, *60*, 153−159.
(27) Bay, L.; Jacobsen, T.; Skaarup, S.; West K. *J. Phys. Chem. B* **2001**, *105*, 8492−7.